Wettability, Saturation, and Viscosity From NMR Measurements

R. Freedman, SPE, and **N. Heaton,** SPE, Schlumberger; **M. Flaum,** SPE, and **G.J. Hirasaki,** SPE, Rice U.; and **C. Flaum,** SPE, and **M. Hürlimann,** Schlumberger-Doll Research Center

Summary

This paper discusses a new nuclear magnetic resonance (NMR) method that can provide wettability, saturation, and oil viscosity values in rocks partially saturated with oil and brine. The method takes advantage of two new technological advances in NMR well logging—the MRF* Magnetic Resonance Fluid Characterization Method and NMR "diffusion-editing" (DE) pulse sequences. We discuss the principles underlying the fluid characterization method and the pulse sequences. The fluid characterization method is used to provide robust inversions of DE data suites acquired on fully brine-saturated and partially saturated rock samples. The outputs of the inversion are separate diffusion-free brine and oil T_2 distributions for the fluids measured in the rocks.

NMR measurements on partially saturated rocks are sensitive to wettability because of surface relaxation of the wetting-phase fluid. The surface relaxation rate, however, must be significant compared to the bulk relaxation rate in order for wettability to noticeably affect the NMR response. We present results showing that the surface relaxation rate at lower wetting-phase saturations is enhanced compared to that measured at higher saturations. The consequence of wetting-phase saturation on NMR-based wettability determination is discussed. Wettability affects the relaxation rates of both the wetting and nonwetting phases in partially saturated rocks. Surface relaxation of the wetting phase in a rock results in shorter relaxation times than would otherwise be observed for the bulk fluid. The nonwetting-phase fluid molecules do not come into contact with the pore surfaces, and therefore their relaxation rate in the rock is the same as in the bulk fluid.

We present accurate and robust computations of diffusion-free T_2 relaxation time distributions for both the wetting and nonwetting phases in four rocks that include two sandstones and two dolomites. A DE data suite was acquired on each rock, measured in two different partial saturation states and also fully brine-saturated. Wettability is determined by comparing the oil and brine T_2 relaxation-time distributions measured in the partially saturated rocks with the bulk oil T_2 distribution and with the T_2 distribution of the fully brine-saturated sample. The brine and oil T_2 distributions are used to compute saturation and oil viscosity values.

A general discussion elucidating the sensitivity range and T_2 limits of diffusion-based NMR methods is given in the appendix. The appendix also derives and displays the gain in signal-to-noise ratio that is achieved by using DE data sequences for fluid characterization in place of Carr-Purcell-Meiboom-Gill (CPMG) data suites.

Introduction

This paper discusses a new NMR method for determining wettability, saturation, and viscosity values in partially saturated reservoir rocks. It has potential applications to wettability interpretation in native-state cores measured in the laboratory as well as to measurements made downhole by an NMR logging tool. Previous methods for determining wettability of partially saturated rocks, including NMR methods, are limited to laboratory measurements.

NMR wettability determination of partially saturated rocks is based on comparing either T_1 or diffusion-free T_2 distributions of oils measured in rocks with the distributions measured on the bulk oils (i.e., outside the rocks). Previous NMR methods of measuring rocks partially saturated with water and oil are only capable of measuring the composite T_2 distribution of both the water and oil phases in the rock. The oil distribution is sometimes measured in restored-state cores by replacing the water phase by D_2O (heavy water), which does not have an NMR signal at the proton Larmor frequency. The latter approach works well but is not useful for studying native-state cores in the laboratory or for downhole NMR measurements.

We take advantage of recent innovations in NMR well-logging technology that provide the capability to measure robust and accurate diffusion-free brine and oil T_2 distributions in partially saturated rocks. These innovations are the MRF characterization method and DE pulse sequences.[1–4] The innovations are discussed in detail in the following sections.

The experiments reported on in this paper were conducted at the Schlumberger-Doll Research (SDR) Center. The NMR data were acquired at a proton Larmor frequency of 1.764 MHz in a magnetic field gradient of 13.2 g/cm.

The experiments included measurements on four rocks— Bentheim and Berea sandstones, and two dolomite samples from the Yates oil field in west Texas. The samples were partially saturated with a 33°API gravity North Sea stock tank oil. The samples were measured first fully brine saturated and then at two partial saturations. The first partial saturation state was at very high oil saturation achieved by drainage of the brine phase close to residual water saturation. The second partial saturation state was at a lower oil saturation achieved by spontaneous imbibition of water for the sandstones and forced imbibition for the dolomites.

Wettability. Wettability is the tendency of a fluid to spread on and preferentially adhere to or "wet" a solid surface in the presence of other immiscible fluids.[5] Knowledge of reservoir wettability is critical because it influences important reservoir properties including residual oil saturation, relative permeability, and capillary pressure. An understanding of the wettability of a reservoir is crucial for determining the most efficient means of oil recovery. This is becoming increasingly important as more secondary and tertiary recovery projects are being undertaken to recover remaining reserves after primary production. It is generally believed that most reservoirs are water-wet or mixed-wet. The concept of mixed wettability was first introduced by Salathiel.[6] In mixed-wet rocks, the brine phase occupies the smaller pores, which are therefore water-wet. In the larger oil- and brine-filled pores, the oil wets part of the pore surfaces.

Two widely used laboratory indicators of wettability are contact angles measured in water-oil-solid systems and the Amott wettability index. The definition of contact angles and their relationship to wettability is shown in **Fig. 1.** Contact angles less than 90°, measured relative to the water phase, are indicative of a preferentially water-wet surface, whereas angles greater than 90° indicate a preferentially oil-wet surface. A practical limitation of contact angle measurements is that they are restricted to special geometries and cannot be made on reservoir rocks.

The Amott wettability index is determined from the amount of oil displaced from a core, starting at some initial oil saturation, by spontaneous imbibition of brine divided by the amount of oil dis-

* Mark of Schlumberger

This paper (SPE 87340) was revised for publication from paper SPE 77397, presented at the 2002 SPE Annual Technical Conference and Exhibition, San Antonio, 29 September–2 October. Original manuscript received for review 9 January 2003. Revised manuscript received 18 June 2003. Manuscript peer approved 8 September 2003.

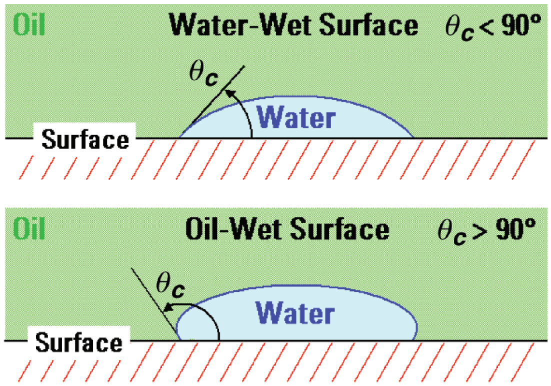

Fig. 1—The definition of wettability of a brine-oil-solid surface according to the contact angle. If θ_c<90°, water exhibits an affinity for the surface that is said to be preferentially water-wet. If θ_c=0°, the surface is strongly water-wet. If θ_c>90°, water exhibits an aversion for the surface that is said to be preferentially oil-wet. If θ_c=180°, the surface is strongly oil-wet.

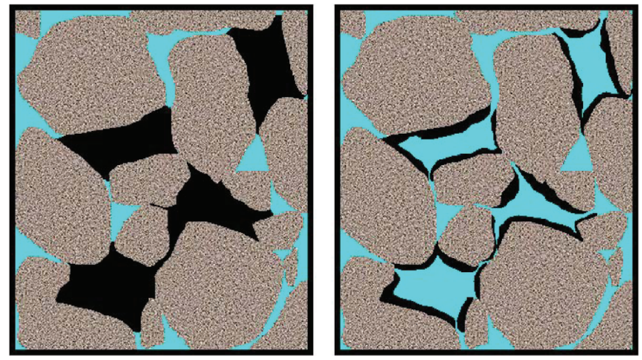

Fig. 2—The fluid distributions in a hypothetical mixed-wet rock at initial oil saturation (left) and after waterflood residual oil saturation (right). The small pores contain only water and are therefore water-wet. The larger oil- and brine-filled pores are oil-wet. For the residual oil saturation shown on the right, the volume occupied by the oil (V_{eff} in Eq. 1) is small compared with a pore volume. This results in enhanced surface relaxation of the oil compared with the same brine-oil-rock system at higher oil saturation.

placed by both spontaneous and forced imbibition.[7] Amott defined an analogous index by also considering the displacement of water by oil. The Amott indices vary linearly on a scale from 0 to 1. The endpoints for the displacement of oil by water are 0 for a neutral to oil-wet system, and 1 for a strongly water-wet system. Imbibition measurements like the Amott index provide the most quantitative indicators of wettability; however, they are limited to the laboratory.

NMR measurements on fluid-saturated porous media are sensitive to wettability because of the enhanced relaxation rate caused when fluid molecules come into contact with pore surfaces that contain paramagnetic ions or magnetic impurities. Surface relaxation of nuclear magnetism is usually the dominant relaxation mechanism for the wetting phase in a partially saturated rock. The nonwetting phase is unaffected by surface relaxation because the pore surface is coated by the wetting fluid. The other relaxation mechanisms, bulk and diffusion relaxation, affect both the wetting and nonwetting phases. The relaxation rate of the transverse magnetization measured in a spin-echo experiment is the sum of the relaxation rates from all three mechanisms. The bulk relaxation rates for liquids are proportional to their viscosities.

The surface relaxation rate of the wetting-phase in a single pore can be written in the form

$$\frac{1}{T_{2,\mathrm{surf}}} = \frac{\rho_2 S}{V_{\mathrm{eff}}}, \quad \text{(1)}$$

where S = the surface area of the pore contacted by the fluid of interest, and ρ_2 = the surface relaxivity, a parameter that accounts for the effectiveness of the surface in promoting spin-relaxation. V_{eff} = the volume occupied by the wetting-phase fluid. It can be considerably less than the pore volume, especially at low wetting-phase saturations. Therefore, in partially saturated rocks, surface relaxation does not depend simply on pore size and surface relaxivity; it is also a function of fluid saturation. For example, in a mixed-wet reservoir at low or residual oil saturation, the surface relaxation of the oil is enhanced, compared to that at higher oil saturations, because of the reduced value of V_{eff}. Eq. 1 and the discussion regarding the dependence of the surface relaxation effect on oil saturation in a mixed-wet rock have relevance to the experimental results discussed later in this paper. **Fig. 2** shows hypothetical fluid distributions in a mixed-wet rock at initial oil saturation, and at after-waterflood residual oil saturation.

Summary of Previous NMR Wettability Studies. It is clear from the previous discussion that the effects of wettability on NMR surface relaxation can be used to provide information on the wettability state of a fluid-saturated rock.

The first publication using NMR measurements to study wettability was a paper by Brown and Fatt,[8] who made T_1 relaxation measurements on water-saturated unconsolidated sandpacks constructed with different fractions of water-wet and oil-wet sand grains. Numerous studies on the application of NMR to wettability have been published since the 1950s. A discussion of many of these papers can be found in the recent paper by Zhang *et al.*[9] Many of the previous studies were conducted on artificial unconsolidated formations.

Studies of wettability of partially saturated reservoir rocks have been mostly limited to rocks saturated with brine and low viscosity hydrocarbons such as Soltrol, decane, and dodecane. Using these low viscosity fluids with narrow T_1 and T_2 distributions and long relaxation times makes it easier to distinguish the hydrocarbon peak from the brine signal in the relaxation-time distributions of partially saturated rocks. Thus, by comparison of the hydrocarbon relaxation times in the rocks with those of the bulk hydrocarbon (i.e., outside the rock), one can infer whether the oil is wetting the surface. One of the shortcomings of these experiments is that wettability inferred from experiments using refined or pure hydrocarbons is not indicative of the wettability of the same rocks saturated with crude oil. In fact, crude oils that contain asphaltenes and resins are well known to have surface-active polar molecules that are attracted to opposite charge sites on the pore surfaces.

Zhang *et al.*[9] measured the T_1 distributions of Bentheim, Berea, and North Burbank sandstone rocks using both a 30°API deepwater Gulf of Mexico crude oil and Soltrol as the nonaqueous saturating fluids. This particular crude oil is known to alter wettability in restored-state core analysis. To separate the oil phase from the brine phase in the measured T_1 distributions, the water in the rock was replaced by diffusing D_2O (heavy water) into the samples. Because D_2O does not have an NMR signal at the proton Larmor frequency, the signal from only the oil phase in the rock was measured.

Zhang *et al.*[9] found that all three sandstones were water-wet when saturated with crude oil and measured at residual water saturation. However, after being aged for 3 weeks at 50°C, the wettability of the samples was changed from water-wet to mixed-wet. After aging, the oil peaks for all three samples were shifted to lower relaxation times. Leu *et al.*[10] have recently used high-field NMR spectroscopy and magic angle spinning to study wettability in native-state cores. The proton chemical shift spectrum of the fluids in the rock can be resolved by spinning the sample to average out the line-broadening field inhomogeneities that otherwise smear out the spectrum. The relaxation-time distributions of the brine and oil in the rock are separately measured while spinning the sample. This method has value for laboratory work but is not suitable for downhole wettability measurements.

Fluid Characterization Method. The new diffusion-based fluid characterization method has been discussed in three recently pub-

lished papers.[1–3] This method exploits the well-known fact that the decay of the transverse magnetization measured in a spin-echo experiment is caused, in part, by molecular diffusion of the fluid molecules. Diffusion of molecules in an inhomogeneous static magnetic field causes the Larmor precession frequencies of the spins to become time-dependent. This leads to imperfect refocusing of the spin-echo signals by the 180° pulses and therefore to an irreversible diffusion-induced decay of the echoes. The diffusion decay rate of the transverse magnetization contributed by freely diffusing molecules that contain hydrogen nuclei is given by

$$\frac{1}{T_{2,\text{diff}}} = \frac{\gamma^2 g^2 t_e^2 D}{12}, \quad (2)$$

where the proton gyromagnetic ratio is represented by $\gamma = 2\pi \cdot 4258$ Hz/Gauss, g = the magnetic field gradient, t_e = the echo spacing, and D = the molecular diffusion coefficient.

The fluid characterization method performs simultaneous inversions of suites of diffusion-encoded spin-echo sequences. The forward model used for the inversions is a multifluid relaxation model that, in general, includes contributions to the spin-echo signals from all the fluids that might be present in the rock pore spaces. The inversion provides diffusion-free brine and crude-oil T_2 distributions that are used to compute total porosity, bulk volume irreducible water, fluid saturations and volumes, oil viscosity, and hydrocarbon-corrected permeability.

The multifluid relaxation model incorporates a constituent viscosity model (CVM) that relates, on a molecular level, diffusion coefficient distributions (D) to relaxation-time distributions (T_1 and T_2) in live and dead crude oils. The correlation between distributions of relaxation times and molecular diffusion coefficients is used to constrain the inversion. The CVM was validated in experiments on hydrocarbon mixtures including live and dead crude oils.[1] The constrained inversion leads to more robust and accurate computations of both brine and crude-oil T_2 distributions in partially saturated rocks than would otherwise be possible.

In the original MRF papers, diffusion information was encoded using suites of CPMG sequences having different echo spacings.[1,2]

DE Pulse Sequences. A recent paper by Hürlimann *et al.*[4] introduced, among other things, a new type of DE spin-echo sequence tailored for fluid typing. DE sequences are similar to CPMG sequences, except that the initial two echoes are acquired with long echo spacings, whereas the third and subsequent echoes are acquired with the shortest possible echo spacing. Diffusion information is encoded during acquisition of the first two echoes, whereas the third and subsequent echoes provide bulk and surface relaxation time information at long acquisition times with little if any attenuation of the signal by diffusion. In contrast, a CPMG sequence acquired with long echo spacing provides poorer bulk and surface relaxation time information, because diffusion decay attenuates the signal after relatively few echoes. A suite of data consisting of DE sequences acquired with different values for the initial two echo spacings provides diffusion information and improved signal-to-noise ratio compared to an analogous suite of CPMG sequences. The increased sampling density for the third and subsequent echoes in a DE sequence, compared to the sparser sampling in a CPMG sequence with long echo spacing, is the reason for the superior signal-to-noise ratio of a DE sequence. A quantitative comparison of the sequences is presented in the Appendix. DE sequences provide more accurate and robust computations of brine and oil T_2 distributions in partially saturated rocks than was previously possible. By accurately measuring crude oil T_2 distributions in a rock and comparing the oil distribution with one measured on the bulk fluid, one can infer the wettability state of the rock. A suite of three DE sequences with different echo spacings for the initial two echoes is shown in **Fig. 3.**

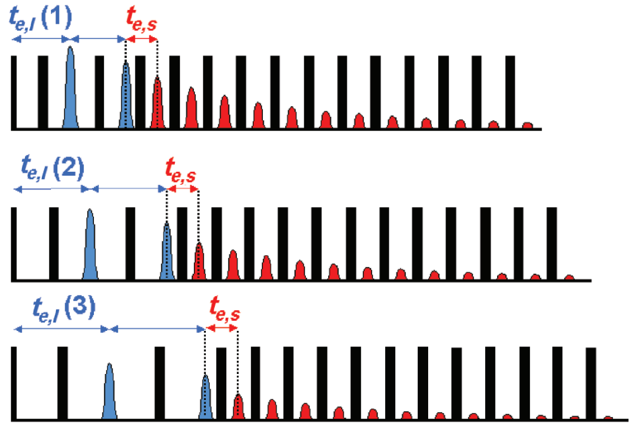

Fig. 3—A suite of three fluid typing DE pulse sequences, each having different initial echo spacings ($t_{e,l}$) for the first two echoes. The third and subsequent spin echoes are acquired with the shortest echo spacing possible ($t_{e,s}$).

MRF Relaxation Model With DE Sequences

This section of the paper discusses the MRF multifluid relaxation model for DE pulse sequences. For the applications in this paper, we consider a two-fluid MRF model with brine and crude oil. The decay of the transverse magnetization, $M(t)$, measured by a DE sequence can be written for a two-fluid model in the general form

$$M(t,t_{e,l}) \approx \sum_{f=o,w} \iiint dD\,dT_1\,dT_2$$

$$\left[P_f(D,T_1,T_2) \exp\left(-\frac{t}{T_2}\right) I(t,t_{e,l},D) f(W,T_1) \right]. \quad (3)$$

The sum is over the two fluids, water and oil. $P_f(D,T_1,T_2)$ is the three-dimensional (3D) diffusion-relaxation time distribution function for each fluid. The function $f(W,T_1)$ corrects for insufficient recovery time (W) between DE sequences, for instance

$$f(W,T_1) = 1 - \exp\left(-\frac{W}{T_1}\right). \quad (4)$$

The exponential T_2 decay factor in the integral includes surface relaxation for the wetting-phase fluid and bulk relaxation for both fluids. The diffusion kernel for the third and subsequent echoes in the DE sequence was discussed by Hürlimann *et al.*[4] and is given by

$$I(t,t_{e,l},D) = \left\{ a_d \exp\left(-\frac{\gamma^2 g^2 D t_{e,l}^3}{6}\right) + a_s \exp\left(-\frac{\gamma^2 g^2 D t_{e,l}^3}{3}\right) \right\}$$

$$\times \exp\left(-\frac{\gamma^2 g^2 D t_{e,s}^2 t}{12}\right) \times \exp\left(\frac{\gamma^2 g^2 D t_{e,s}^2 t_{e,l}}{6}\right) \quad (5)$$

for $t > 2t_{e,l}$, where $t_{e,l}$ = the echo spacing for the initial two echoes (see Fig. 3) and $t_{e,s}$ = the short echo spacing for the third and subsequent echoes in a DE sequence. The factor containing $t_{e,s}$ in Eq. 5 accounts for any diffusion-decay occurring during the acquisition of the third and subsequent echoes. Hürlimann[11] has shown that diffusion decay in an inhomogeneous magnetic field is biexponential, with the two contributions coming from direct and stimulated echoes. The direct and stimulated echo coefficients, a_d and a_s, depend on the receiver bandwidth of the NMR instrument or logging tool. They can be determined by fitting the diffusion kernel in Eq. 5 to a suite of DE data acquired on a water sample. The values used for all computations in this paper were $a_d = 0.88$ and $a_s = 0.04$. The diffusion kernel for the initial two echoes (e.g., for $t \leq 2t_{e,l}$) can be represented, to within a very good approximation, by a single exponential decay factor:

$$I(t,t_{e,l},D) = \exp\left(-\frac{\gamma^2 g^2 D\, t_{e,l}^2 t}{12}\right). \quad (6)$$

Note that if $t_{e,l} = t_{e,s}$ the coefficients, $a_d = 1$ and $a_s = 0$, and therefore, Eqs. 3, 5, and 6, reduce to the expected results for a CPMG sequence with echo spacing $t_{e,s}$. As with CPMG sequences, the first few echoes in a DE sequence are affected by off-resonance

effects. These effects can be corrected by multiplying the first few echoes by spin-dynamics correction factors.

Although it is possible, in principle, to invert the DE data suites and extract the 3D diffusion-relaxation time distribution function in Eq. 3, we use the MRF method. This method takes advantage of correlations between relaxation times and diffusion coefficients for crude oils. This provides a huge simplification of the general forward model for DE sequences in Eq. 3 because it reduces the 3D integral for each fluid to a simple 1D integral over T_2. For example, the 3D diffusion-relaxation time distribution function for crude oils can be written in the form

$$P_o(D,T_1,T_2) = P_o(T_2)\delta(D - \lambda T_2)\delta(T_1 - \xi_o T_2), \quad \ldots\ldots\ldots\ldots (7)$$

where $P_o(T_2)$ = the diffusion-free T_2 distribution of the oil. The 1D distributions for D and T_1 are Dirac delta (δ) functions. The parameter λ in Eq. 7 relates the diffusion and relaxation-time distributions in accordance with the CVM. For many dead crude oils it has been established that an average value of $\lambda \approx 1.25\times10^{-5}$ cm^2/s^2 is appropriate. For live crude oils, λ is multiplied by an empirically determined function of the solution gas/oil ratio. The average value of λ given above is determined from the ratio of two empirically derived correlation parameters that relate the log means of diffusion and relaxation-time distributions in crude oils to viscosity.[1] Because of the approximate nature of empirical correlations, we have found variations in λ for different crude oils on the order of a factor of 2. For the North Sea crude oil used to saturate the samples in our experiments, it was found that the parameter $\lambda = 0.51\times10^{-5}$ cm^2/s^2. If the wrong value of λ is used, then the relaxation model will not fit the data. A poor fit manifests itself in the normalized goodness-of-fit parameter, χ^2, being much greater than 1. The correct value of λ for the North Sea oil was found by searching for the value that gave the minimum χ^2.

The parameter ξ_o in Eq. 7 is the apparent T_1/T_2 ratio of the crude oil. It has been established, for Larmor frequencies of a few MHz or less, that $\xi_o \approx 1$ for many crude oils with low-to-medium viscosities. The T_1/T_2 ratios of crude oils can be greater than 1 for high-viscosity oils and at higher Larmor frequencies because of the breakdown of the fast-motion condition.[1] In mixed-wet rocks, surface relaxation of the oil can also affect and cause deviations of ξ_o from the T_1/T_2 ratio of the bulk oil. For the experiments in this paper, fully polarized data suites were acquired so that there was no T_1 (and therefore ξ_o) dependence. The 3D distribution function for the brine phase can be written in the form

$$P_w(D,T_1,T_2) = P_w(T_2)\ \delta(D - D_w(T))\ \delta(T_1 - \xi_w T_2), \quad \ldots\ldots\ldots (8)$$

where $D_w(T)$ = the temperature-dependent molecular diffusion coefficient of water, and ξ_w = the apparent T_1/T_2 ratio of the water phase in the rock. Substituting Eqs. 7 and 8 into Eq. 3, and using the properties of the Dirac delta functions to perform the integrations over D and T_1, one finds that the MRF relaxation model for DE sequences can be written as the sum of contributions from the water and oil phases; e.g.,

$$M(t,t_{e,l}) \approx \int dT_2 P_w(T_2)\exp\left(-\frac{t}{T_2}\right) I(t,t_{e,l},D_w) f(W,\xi_w T_2) + \int dT_2 P_o(T_2)\exp\left(-\frac{t}{T_2}\right) I(t,t_{e,l},\lambda T_2) f(W,\xi_0 T_2). \quad \ldots\ldots (9)$$

The relaxation model in Eq. 9 was used to invert the suites of DE data for all the experiments discussed in this paper. The details of the inversion follow along the lines previously given by Freedman[12] for suites of CPMG sequences. The inversion provides robust estimates of the water and crude oil T_2 distributions, $P_w(T_2)$ and $P_o(T_2)$.

Before concluding this section, it is useful to discuss briefly restricted diffusion effects on NMR diffusion-based fluid characterization. Diffusion-based NMR fluid characterization methods rely on the existence of a sufficient contrast in the fluid diffusivities to distinguish one fluid from another. The MRF model assumes unrestricted diffusion of the fluid molecules. Although this is an approximation, our experience has shown that bulk diffusion is usually the dominant effect and restricted diffusion is typically, for most rocks, a second-order effect. This is supported by the fact that the MRF method has been shown to provide accurate water saturations in partially saturated rocks over a range of saturations and for a diverse suite of sandstone and carbonate rocks.[2]

Experiments

This section discusses the results of the experiments. We discuss petrophysical properties of the rock samples, crude oil properties, sample preparation, pulse sequences, and the results of the data processing.

Rock and Crude Oil Properties. The sandstones used in the experiments were Bentheim (BEN3) and Berea (BER2). The petrophysical properties of these sandstones are quite different. Bentheim is a virtually clay-free rock that has a very high permeability. Berea sandstone is moderately shaly and known to contain kaolinite and illite clays and some localized siderite flakes.

In addition to the sandstones, our experiments included two dolomite rocks (Y1312 and Y1573) from the Yates field in west Texas. The Yates field dolomites have a complex dual-porosity pore space structure that contains significant amounts of microporosity. The macropores in these rocks include vugs with dimensions on the order of 100 microns. Moreover, these rocks are fractured, and they are known to be mixed-wet from water imbibition experiments. The porosities and permeabilities for the rocks used in the experiments are shown in **Table 1.** Stock-tank oil from a North Sea reservoir was used to partially saturate the samples. The properties of the crude oil are shown in **Table 2.** The measured viscosity of the North Sea crude oil is 9.4 cp at 27°C.

Sample Preparation and DE Data Suite. All the core samples were in the shape of 1-in.-long cylinders with 1-in. diameters. The samples were wrapped in heat-shrinkable Teflon, brine-saturated by vacuum, and then pressurized to remove any air. A suite of DE measurements was performed on these samples at 100% brine saturation. The samples were then submerged in the North Sea crude oil and centrifuged for 11 hours at 3,400 rpm at a capillary pressure of 17 psi. The objective was to achieve a saturation state with relatively high oil saturation. The samples were then inverted, and centrifuged for an additional hour. The samples at this stage were close to, or at, irreducible water saturation, and therefore were at high oil saturations. A second suite of DE measurements was then performed. We will refer to this high oil-saturation state as the drainage state, and use the abbreviation DR in the following figures and tables. At this point, all the samples were submerged in brine for 16 hrs. For the sandstone samples, spontaneous imbibition was observed. For the dolomites, no spontaneous imbibition was observed, and the samples were spun in brine at 3,400 rpm for 1 hr to force imbibition. We will refer to this lower oil saturation state as an imbibition state, and use the abbreviation IM in subsequent figures and tables. A final suite of DE data was acquired on the samples in the imbibition state. The NMR measurements were conducted in the fringe field of a superconducting magnet. A detailed description of the experimental apparatus can be found in Ref. 11. The samples were placed inside a solenoidal coil tuned to the proton Larmor frequency of 1.76 MHz in a constant magnetic gradient of 13.2 g/cm. The temperature of the samples was held constant at 25°C during the measurements.

The full DE measurement suite acquired on each sample consisted of a CPMG with an interecho spacing of 0.4 ms and 11 DE sequences with initial echo spacings of 1.2, 2.4, 4.4, 8.4, 12.4,

TABLE 1—ROCK POROSITIES AND PERMEABILITIES

Sample	Porosity (p.u.)	Air Permeabilities (md)
BEN3	23.4	2960
BER2	19.6	205
Y1312	20.8	137
Y1573	14.2	57

TABLE 2—CRUDE OIL PROPERTIES					
Oil	API Gravity	Wt% Asphaltenes	Wt% Resins	Wt% Aromatics	Wt% Saturates
N. Sea	33.2	0.0	7.9	24.9	67.1

16.4, 20.4, 24.4, 28.4, 32.4, and 36.4 ms. For the DE sequences, the short interecho spacing (e.g., for the third and subsequent echoes) was 0.4 ms. The number of echoes acquired for the CPMG and for each DE sequence was 4002. Thus, a complete suite of measurements for each sample, including the CPMG, consisted of 48,024 echoes. A polarization time of 6 seconds preceded each measurement to provide essentially full polarization of all fluids. The sequences for each acquisition were repeated and averaged to reduce the random noise to approximately 1.0 p.u.

Before discussing the experimental results, it is instructive to pause here and display the DE data suites acquired on one of the rock samples measured partially saturated and fully brine-saturated. These plots provide insight into why DE data suites are so useful for fluid characterization. **Figs. 4 and 5** show the DE suites for Berea sandstone measured fully brine saturated and partially saturated, respectively. Note that the echo amplitudes are in arbitrary units. A porosity calibration of the data was not performed in these experiments, because NMR porosity determination was not one of the objectives of this study. Fig. 4 shows that the water signal decays to the noise level for long initial echo spacings (i.e., $t_{e,l}$) greater than approximately 20.4 ms. The large attenuation decay for long $t_{e,l}$ values is caused by the large diffusion coefficient of the water molecules. By contrast, there is still a signal observed for long $t_{e,l}$ values in the partially saturated Berea sample shown in Fig. 5. This is because the molecular diffusion coefficients of the molecules in this intermediate viscosity oil are roughly an order of magnitude smaller than that of water. This signal is attributed entirely to the oil, because the water signal decays away during the first two echoes for long $t_{e,l}$. One can qualitatively differentiate a rock that contains oil from one that is fully brine saturated simply by the presence or absence of signal at long values of $t_{e,l}$ without any data processing, provided that there is enough contrast between the brine and oil diffusivities.

Fully Brine-Saturated Samples. The T_2 distributions for the North Sea oil and each of the rocks at 100% brine saturation were

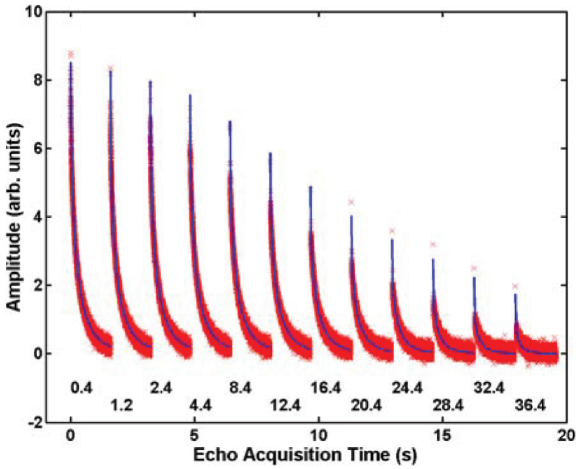

Fig. 5—The full DE data suite acquired on the Berea sandstone measured in the drainage state. The 6-second wait time that preceded each echo acquisition is not shown. The data suite includes a CPMG (the first measurement shown) with an echo spacing of 0.4 ms. Observe that there is observable signal for all the DE measurements. The signal observed at long $t_{e,l}$ values is attributed to oil only because the more rapidly decaying water signal disappears for $t_{e,l}$ values greater than approximately 20.4 ms. The solid lines are the post-inversion fit of the relaxation model to the full DE data suite.

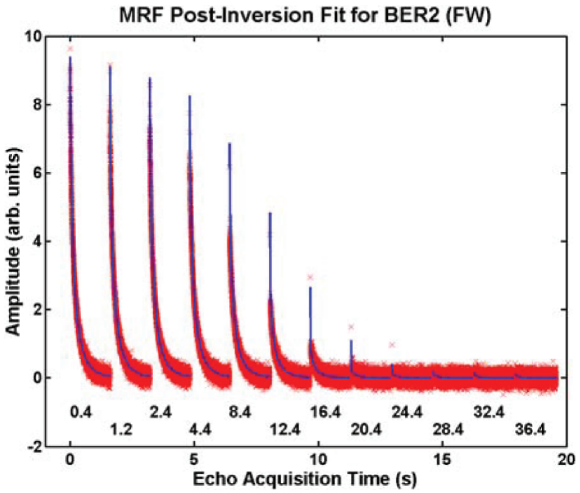

Fig. 4—The full DE data suite acquired on the fully brine-saturated Berea sandstone. The 6-second wait time that preceded each echo acquisition is not shown. The data suite includes a CPMG (the first measurement shown) with an echo spacing of 0.4 ms. Observe that the water signal has decayed to the noise level for $t_{e,l}$ values greater than approximately 20.4 ms. The water signal decays rapidly to the noise level at long $t_{e,l}$ values because of the large diffusion coefficient of water. The fact that no signal is observed for long $t_{e,l}$ values is a good indicator that the sample is water saturated. The solid lines are the post-inversion fit of the relaxation model to the full DE data suite.

first measured using the CPMG sequence. These distributions are shown in **Fig. 6.** Dividing by the peak amplitude in each distribution normalized the amplitudes of each distribution in Fig.6. This makes it easier to compare the distributions from rocks with different porosities. Note that the brine T_2 distributions all strongly overlap the crude oil distribution. This strong overlap of brine and oil T_2 distributions in partially saturated rocks makes it difficult to accurately differentiate and separate brine and oil distributions in the composite T_2 distributions that contain both brine and oil.

Wettability Results for the Partially Saturated Samples. **Fig. 7** shows diffusion-free oil T_2 distributions computed from the fluid characterization method by inversion of the DE data suites acquired for each of the partially saturated rocks in the drainage state.

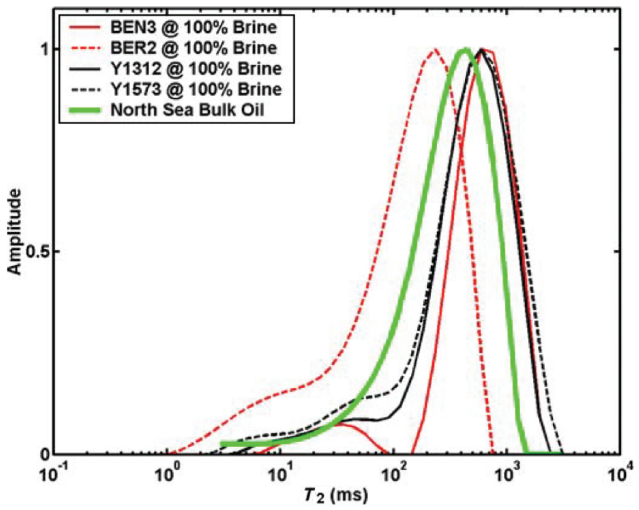

Fig. 6—The T_2 distributions of the North Sea crude oil and the 100% brine-saturated rocks measured using the CPMG sequence. Note the strong overlap of the oil and brine T_2 distributions. It is this overlap between oil and brine T_2 distributions in partially saturated rocks that makes it difficult to accurately separate the oil and brine phases.

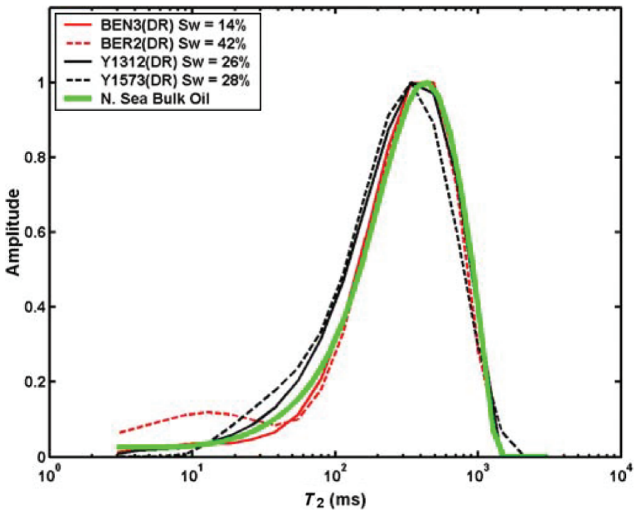

Fig. 7—The diffusion-free oil T_2 distributions computed by the fluid-characterization method for the samples measured in the drainage state compared with the bulk oil distribution. Note that there is no convincing evidence of surface relaxation of the oil phase, even though the two Yates samples are mixed-wet. The surface relaxation rate of the oil is not significant compared to the bulk oil relaxation rate at these high oil saturations.

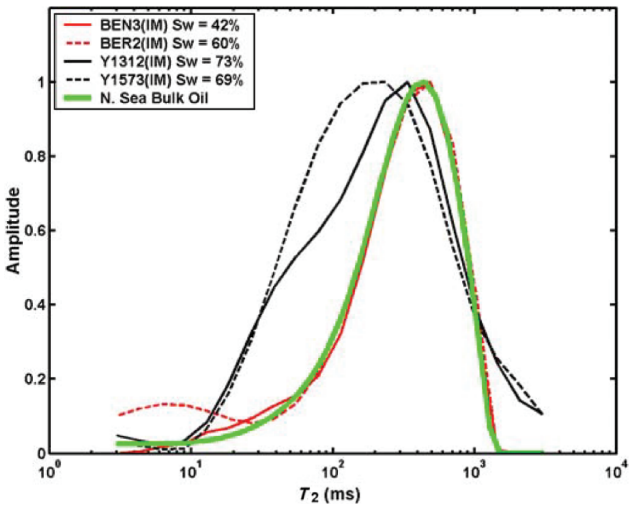

Fig. 8—The diffusion-free oil T_2 distributions computed by the fluid characterization method for the samples measured in the imbibition state compared with the bulk oil distribution. Note that there is convincing evidence of surface relaxation of the oil phase in the two mixed-wet Yates samples.

The computed water saturations are also shown. Also shown is the T_2 distribution of the North Sea bulk oil. The same normalization procedure applied to the brine distributions in Fig. 6 was also applied to the oil distributions shown in Figs. 7 and 8. This makes it easier to compare the shapes and positions of oil T_2 distributions in rocks having different oil volumes. Note that the oil T_2 distribution measured, so to speak, "in each of the rocks" agrees very well with the bulk distribution for the oil measured "outside the rocks." The oil distributions measured in the two Yates samples show a very slight shift to shorter relaxation times. Nevertheless, one would conclude from Fig. 7 that all four of these partially saturated rocks are water-wet, because there is no conclusive evidence of surface relaxation of the oil phase. This conclusion is incorrect, because in fact the two Yates samples are mixed-wet. The reason that surface relaxation of the oil measured in these samples is not evident is that the surface relaxation rate depends on the saturation of the wetting phase, as is discussed in the paragraph that follows Eq. 1. Because measurements were performed at high oil saturations, the surface relaxation rate is apparently too weak in comparison to the bulk relaxation rate to produce an observable effect for these samples.

The dependence of the surface relaxation rate on wetting-phase saturation is evident in **Fig. 8,** which shows computed oil distributions for the samples measured in the imbibition state. In Figs. 7 and 8, note that the water saturations in the imbibition state are significantly higher than those measured after drainage. The oil T_2 distributions measured in the two Yates samples in the imbibition state show a significant shift toward shorter relaxation times. This effect is caused by surface relaxation of the oil in these mixed-wet dolomites that is enhanced because of the higher water saturations. Fig. 8 shows that the oil distributions computed for the two water-wet sandstones, BEN3 and BER2, agree very well with the bulk oil distribution and show no signs of surface relaxation.

It is clear from these results that oil relaxation-time distributions measured in mixed-wet rocks with oil in contact with the pore surface can show signs of significant surface relaxation. However, if no surface relaxation of oil in a rock is observed, one cannot conclude that the rock is water-wet; still, if one observes a significant shift toward short relaxation times of the oil T_2 distribution compared to that of the bulk oil, one can conclude that the rock is mixed-wet. These observations place some qualifications not previously discussed in the literature on the sensitivity of NMR measurements to wettability.

Wettability has an effect on both the wetting and nonwetting fluids in a pore. The relaxation rate of the wetting fluid is increased by surface relaxation at the pore surface, whereas the relaxation rate of the nonwetting fluid should approach its bulk value, because there is no surface relaxation effect. In light of these remarks, it is instructive to compare the computed brine distributions for the samples measured in the imbibition state with those measured fully brine-saturated.

Figs. 9 and 10 show the brine T_2 distributions for the Bentheim and Berea sandstones measured at imbibition and at 100% brine saturation. The brine distributions are consistent with expectations for a water-wet rock. At imbibition, brine and oil occupy the larger pores, and the smaller pores are filled with brine. Because the rock is water-wet, the brine in the larger pores remains in contact with the pore surfaces. The brine relaxation times in the large pores are reduced compared to those of the fully brine-saturated rock, because the effective volume of the brine in the larger pores is reduced (e.g., see Eq. 1) by the presence of the oil.

Figs. 11 and 12 show the brine T_2 distributions for the Yates dolomites measured at imbibition and at 100% brine saturation.

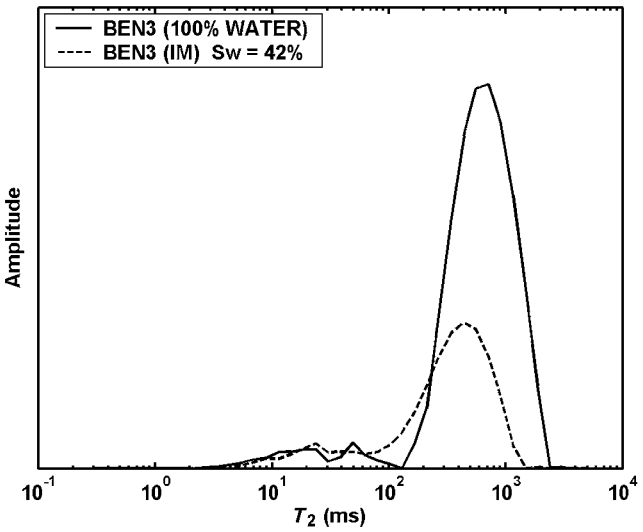

Fig. 9—Comparison of the brine distributions for the Bentheim sandstone, measured fully brine-saturated and in the imbibition state. As discussed in the text, these distributions are consistent with those expected for a water-wet rock.

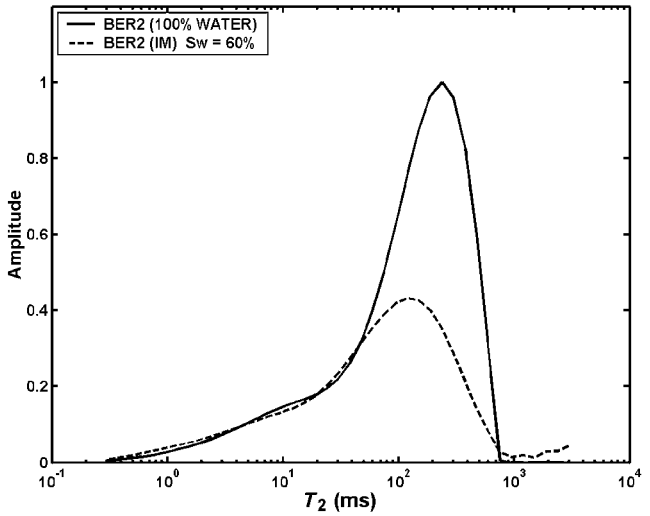

Fig. 10—Comparison of the brine distributions for the Berea sandstone, measured fully brine-saturated and in the imbibition state. As discussed in the text, these distributions are consistent with those expected for a water-wet rock.

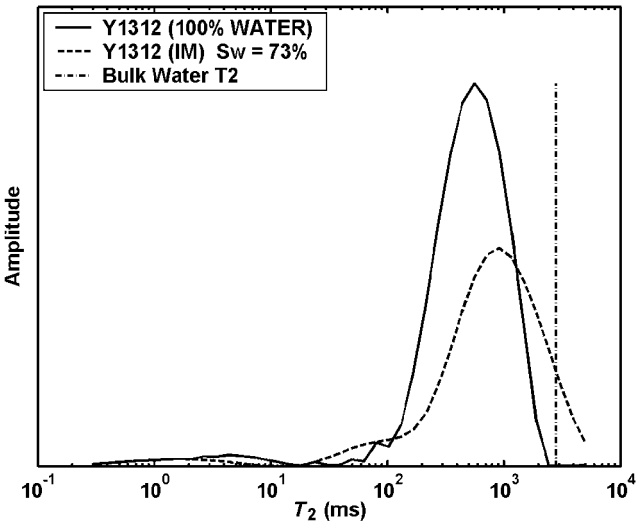

Fig. 11—Comparison of the brine distributions for the Y1312 dolomite sample, measured fully brine-saturated and in the imbibition state. Note that some of the brine in the large oil- and brine-filled pores is not in contact with the pore surfaces, and therefore relaxes close to its bulk rate. In the fully brine-saturated state, the brine relaxation times in the large pores are reduced compared to that of bulk brine by surface relaxation.

The brine distributions for these rocks measured in the imbibition state are consistent with those of a mixed-wet rock with brine occupying the small pores and oil wetting the pore surfaces in the larger pores (e.g., see Fig. 2). In the imbibition state, the brine in the larger pores does not contact the pore surfaces, and therefore relaxes with its bulk relaxation time. This is exactly the behavior observed in Figs. 11 and 12. Note how the centers of the brine distributions measured at imbibition are shifted to longer relaxation times. This behavior is quite different from that observed in Figs. 9 and 10 for the water-wet sandstones.

Saturation and Viscosity Results. **Table 3** lists some results obtained from MRF processing of the DE data suites for each of the 8 partially saturated samples measured in this study. Column 1 lists the samples, and shows the saturation state at which each measurement was performed. Column 2 lists the computed water saturations. Column 3 lists the log means of the computed oil T_2 distributions. The log mean of the T_2 distribution of the North Sea bulk oil sample is 288 ms, and the measured viscosity at 27°C is 9.4 cp. The log means of the oil distributions in the partially saturated samples are, except for Y1312 (IM) and Y1573 (IM), in good agreement with that of the bulk oil. Differential weight measurements (DWM) of water saturation were not performed for the samples in this study. In a recently published paper,[2] we showed good agreement between MRF estimated water saturations and those from DWM for a suite of rocks that includes those used in this study. **Fig. 13** shows the estimated viscosities that are derived from the log means using an empirical correlation.[1] The agreement with the measured viscosity is very good except for the two Yates samples measured at imbibition. For these two mixed-wet samples, surface relaxation reduces the log mean relaxation times compared to that of the bulk oil and causes overestimation of the viscosity. For the North Sea oil used in these experiments, the empirically derived parameter that relates the log mean of the oil distribution to viscosity is equal to 0.0087 $s \cdot cp \cdot K^{-1}$, which is 2.17 times greater than the default value frequently used for crude oils.[1] Also, the parameter that relates oil diffusion coefficients to relaxation times in the CVM has the value $\lambda = 0.51 \times 10^{-5}$ cm^2/s^2, which also deviates from the default value. Column 4 lists the normalized goodness-of-fit parameter (χ^2) computed after the inversion. A value equal to 1.0 (or less) indicates a perfect fit to within noise errors.

The correlation between D and T_2 in Eq. 7 was developed for bulk crude oils. In mixed-wet rocks, with significant surface relaxation of the oil phase, the T_2 values of the oil can be substantially reduced compared with their bulk values. If the diffusion constants remained unchanged, this would imply a deviation from

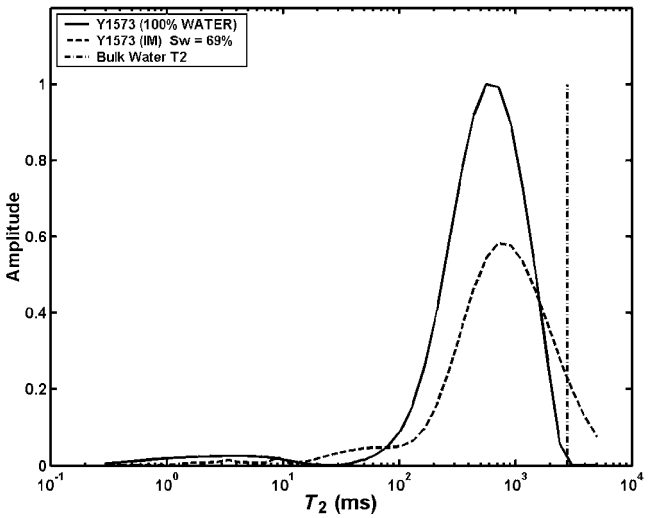

Fig. 12—Comparison of the brine distributions for the Y1573 dolomite sample, measured fully brine-saturated and in the imbibition state. Note that some of the brine in the large oil- and brine-filled pores is not in contact with the pore surfaces and therefore relaxes close to its bulk rate. In the fully brine-saturated state, the brine relaxation times in the large pores are reduced compared to that of bulk brine by surface relaxation.

TABLE 3—PROCESSING RESULTS FOR PARTIALLY SATURATED SAMPLES

Sample	S_W (%)	$T_{2O,LM}$ (ms)	χ^2
BEN3 (DR)	13.8	297	0.97
BER2 (DR)	42.0	257	1.06
Y1312 (DR)	26.1	243	1.02
Y1573 (DR)	28.4	235	0.99
BEN3 (IM)	42.4	273	0.99
BER2 (IM)	60.3	266	1.06
Y1312 (IM)	73.3	155	1.01
Y1573 (IM)	69.1	147	1.01

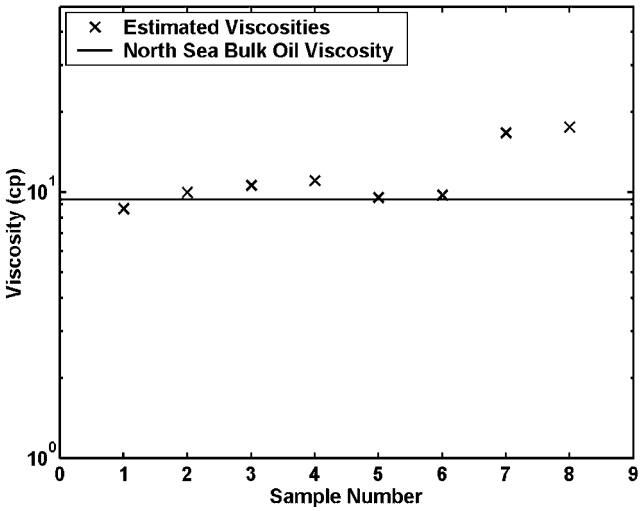

Fig. 13—The estimated viscosities for the eight partially saturated samples listed in Table 3. The sample number on the *x*-axis is consistent with the order in which the samples are listed in Table 3. The good agreement with the measured bulk oil viscosity for Samples 1 through 6 is because of accurate estimations of the T_2 distributions of the oil in the rocks and the absence of significant surface relaxation effects. The overestimation of the viscosity for the two Yates samples measured at imbibition is caused by the significant surface relaxation of the oil in these mixed-wet rocks.

the bulk oil correlation. The fact that the model provides a good fit to the data in the mixed-wet rocks, Y1312 (IM) and Y1573 (IM), suggests that the oil diffusion constants are also reduced. Apparently, at high water saturations, the oil molecules are trapped in the thin layers between the grain surfaces and the oil/water interfaces and experience restricted diffusion. As was shown in a recent publication,[2] the model provides estimates of fluid saturations in mixed-wet Yates dolomite rocks that compare very well with saturations determined from gravity measurements.

Table 4 shows estimated water saturations and normalized goodness-of-fit parameters for the samples measured in the fully brine-saturated state. The notation FW is used to indicate that the samples were fully brine-saturated. The underestimation (i.e., by a few saturation percent) of the water saturations in the sandstone samples is caused by model and data errors. This is within the expected accuracy limits of the technique. The bigger underestimation of the water saturation in the Yates samples is caused, in part, by restricted diffusion of the brine molecules in the microporosity. Restricted diffusion can cause water trapped in the micropores to be mistaken for oil molecules. For these molecules, the apparent diffusion coefficients are reduced and clearly depend on the sizes of the micropores, and therefore on their T_2 values. Because our experiments were conducted in a low magnetic field gradient (i.e., 13.2 g/cm), DE sequences having long diffusion times (e.g., 2 $t_{e,l}$) were required in order to accurately separate the oil and water signals. Long diffusion times imply long diffusion lengths, which exacerbate restricted diffusion effects. The effects of restricted diffusion can be reduced significantly by using larger field gradients and shorter diffusion times. Another reason for errors in the water saturation is the lack of diffusion sensitivity at very short relaxation times that makes it impossible to reliably differentiate water in micropores from fast-relaxing large molecules in crude oils.

TABLE 4—PROCESSING RESULTS FOR FULLY BRINE-SATURATED SAMPLES

Sample	S_W (%)	χ^2
BEN3 (FW)	95.7	0.97
BER2 (FW)	96.2	1.10
Y1312 (FW)	91.7	1.03
Y1537 (FW)	83.2	1.02

Conclusions

This paper discusses a new NMR method for measuring wettability, saturation, and viscosity in rocks partially saturated with brine and crude oils. The method has advantages over existing methods for inferring wettability. Specifically, the method presented here is applicable to analysis of native-state cores and also to in-situ wettability determination.

The dependence of NMR surface relaxation on the wetting-phase saturation was discussed and demonstrated using data acquired from two mixed-wet dolomite samples, each measured in two different saturation states.

It was shown that suites of DE pulse sequences provide enhanced signal-to-noise ratios compared to comparable suites of CPMG data.

It was also shown how DE data suites can be used with the magnetic resonance fluid characterization method to compute accurate oil and brine T_2 distributions in partially saturated rocks. The capability to compute accurate oil and brine T_2 distributions of oil in rocks leads to a new technique for inferring mixed-wettability. The basis of the method is a comparison of the oil T_2 distribution measured in a partially saturated rock with the bulk oil (e.g., measured outside of the rock) T_2 distribution. A significant shortening of the relaxation times of the oil distribution measured in the rock compared to the bulk oil distribution provides unambiguous evidence of surface relaxation of the oil (i.e., the rock is mixed-wet). In the large pores where the oil is wetting the pore surfaces, the brine molecules do not contact the pore surfaces and, therefore, experience reduced surface relaxation. As a result, the brine T_2 values in the large pores will be shifted toward longer T_2 values compared to those in the fully water-saturated rock, and should approach the bulk water value.

The enhanced relaxation rate of the oil and the concomitant reduced brine relaxation rate were demonstrated in two mixed-wet dolomite samples measured in states with moderate oil saturations. It was also shown that the oil T_2 distributions in the same two mixed-wet dolomite rocks measured in states with very high oil saturations do not exhibit reduced relaxation times compared to the bulk oil distribution. Thus, NMR measurements can be used to infer mixed-wettability only if one observes a surface relaxation effect on the oil in the rock. If no surface relaxation effect on the oil measured in the rock is observed, then the wettability of the rock cannot be inferred from NMR. An advantage of our method over previous wettability methods is that it can be adapted to study in-situ wettability. The technique should be best suited to reservoirs with low-to-moderate oil saturations.

Nomenclature

a_d = amplitude of direct echo contribution (see Eq. 5)
a_s = amplitude of stimulated echo contribution (see Eq. 5)
D = diffusion coefficient, $cm^2 \cdot s^{-1}$
$E(V_o,V_w)$ = error function
g = applied magnetic field gradient, g/cm
$I(t,t_{e,l},D)$ = diffusion kernel for DE pulse sequence (see Eqs. 5 and 6)
j = integer index that denotes echo number
M_k = amplitude of measured transverse magnetization
$M(t,t_{e,l})$ = transverse magnetization in DE sequence, p.u.
p = integer index that denotes measurement number in a suite of DE measurements
$P(D,T_1,T_2)$ = 3D diffusion-relaxation time distribution, (p.u.)$\cdot cm^{-2} \cdot s^{-1}$
$P(T_2)$ = T_2 distribution, (p.u.) $\cdot s^{-1}$
S = surface area of a pore in contact with the wetting fluid of interest, cm^2
t = echo acquisition time, sec

t_e = echo spacing, sec
$t_{e,l}$ = long echo spacing for initial two echoes in DE sequence, sec
$t_{e,s}$ = short echo spacing for third and subsequent echoes in DE sequence, sec
T_1 = longitudinal relaxation time, sec
T_2 = diffusion-free spin-spin relaxation time caused by surface and bulk relaxation, sec
$T_{2,\mathrm{diff}}$ = spin-spin relaxation time caused by molecular diffusion in the applied magnetic field gradient, sec
$T_{2,\mathrm{surf}}$ = spin-spin relaxation time caused by surface relaxation, sec
V_{eff} = volume of the wetting phase in a rock pore, cm^3
W = wait time preceding a DE or CPMG measurement, sec
γ = proton gyromagnetic ratio, $(\mathrm{Gauss}\cdot\mathrm{s})^{-1}$
δ = Dirac delta function
λ = parameter that relates diffusivity and relaxation time in a crude oil, $\mathrm{cm}^2\cdot\mathrm{s}^{-2}$
ξ = apparent T_1/T_2 ratio of of oil or water
ρ_2 = T_2 surface relaxivity, $\mathrm{cm}\cdot\mathrm{s}^{-1}$
χ^2 = normalized goodness-of-fit parameter used to assess how well the MRF relaxation model fits the DE data suite

Subscripts

f = oil or brine
o = oil
w = brine

Acknowledgments

We thank Drs. Francois Auzerais and Martin Poitzsch for supporting this study. We are also grateful to the oil companies that provided the core and oil samples used in the experiments.

References

1. Freedman, R. *et al.:* "A New NMR Method of Fluid Characterization in Reservoir Rocks: Experimental Confirmation and Simulation Results," *SPEJ* (December 2001) 452.
2. Freedman, R., Heaton, N., and Flaum, M.: "Field Applications of a New Nuclear Magnetic Resonance Fluid Characterization Method," *SPEREE* (December 2002) 455.
3. Heaton, N., *et al.:* "Applications of a New-Generation NMR Wireline Logging Tool," paper SPE 77400 presented at the 2002 SPE Annual Technical Conference and Exhibition, San Antonio, Texas, 29 September–2 October.
4. Hürlimann, M.D. *et al.:* "Diffusion-Editing: New NMR Measurement of Saturation and Pore Geometry," paper FFF presented at the 2002 Annual Meeting of the Society of Professional Well Log Analysts, Oiso, Japan, 2–5 June.
5. Craig, F.F.: *The Reservoir Engineering Aspects of Waterflooding*, Monograph Series, SPE, Richardson, Texas (1971) **3.**
6. Salathiel, R.A.: "Oil Recovery by Surface Film Drainage In Mixed-Wettability Rocks," *JPT* (October 1973) 1216; *Trans.,* AIME, **255.**
7. Amott, E.: "Observations Relating to the Wettability of Porous Rock," *Trans.,* AIME (1959) **216,** 156.
8. Brown, R.J.S. and Fatt, I.: "Measurements of Fractional Wettability of Oilfield Rocks by the Nuclear Magnetic Relaxation Method," *Trans.,* AIME (1956) **207,** 262.
9. Zhang, Q., Huang, C.C., and Hirasaki, G.J.: "Interpretation of Wettability in Sandstones With NMR Analysis," *Petrophysics* (May–June 2000) **41,** No. 3, 223.
10. Leu, G. *et al.:* "NMR Identification of Fluids and Wettability in Situ in Preserved Cores," *Petrophysics* (January–February 2002) **43,** No. 1, 13.
11. Hürlimann, M.D.: "Diffusion and Relaxation Effects in General Stray Field NMR Experiments," *J. Magn. Res*. (2001) **148,** 367.
12. Freedman, R.: "Formation Evaluation Using Magnetic Resonance Logging Measurements," U.S. Patent No. 6,229,308 B (2000).

Appendix—T_2 Sensitivity Limits of NMR-Based Fluid Characterization and Comparison of DE and CPMG Data Suites

The fluid characterization method relies on the fact that signals from water and crude oil usually have different diffusion attenuation rates because of contrasts in their molecular diffusion coefficients. The method also requires that the NMR signal relaxation rate caused by diffusion is significant in comparison to other relaxation processes (i.e., surface and bulk relaxation). The latter requirement is not satisfied for very viscous oils or for very fast-relaxing brine signals for which there can be negligible sensitivity to diffusion relaxation. This lack of diffusion information means that NMR cannot reliably differentiate fast-relaxing water in small pores or clay-bound waters from heavy constituents in crude oils that also have very short relaxation times. This limitation applies to all NMR-based diffusion methods and was discussed in a previous paper.[2] At the other end of the spectrum, NMR diffusion methods cannot reliably differentiate bulk water in large pores from very low-viscosity oils with similar diffusion coefficients. In the latter cases, the problem is not attributable to insignificant diffusion relaxation. Indeed, for both light oils and bulk water, the diffusion attenuation rates are high. The problem is caused by lack of contrast between the diffusion coefficients of very low-viscosity oils and water.

In this Appendix, we quantify the aforementioned limits by a simple sensitivity analysis of the errors in the volume estimates of water and crude oil in a partially saturated rock. The computations also show that suites of DE sequences provide more robust and accurate fluid volumes than can be obtained using suites of CPMG sequences.

To simplify the computations, we will assume that the rock is water-wet and that the measurements are all fully polarized. Consider a fixed value of T_2 caused by bulk and surface relaxation for the water and by bulk relaxation for the oil. Consider a suite of DE sequences, and let M_k be the amplitude of the measured transverse magnetization. To save space, we have introduced the dual-index $k=(j,p)$, where $j=$the echo number and p denotes a DE sequence in the measurement suite. In the following analysis, summations over the index k are understood to be a double summation over all echoes in each sequence and then over all sequences in the suite. On using Eq. 9, the measured magnetization M_k for the jth echo and pth DE sequence can be written in the form

$$M_k = V_{\mathrm{o}} \exp\left(-\frac{jt_{e,k}}{T_2}\right) I(k,\lambda T_2) + V_{\mathrm{w}} \exp\left(-\frac{jt_{e,k}}{T_2}\right) I(k,D_w(T)], \quad \text{.....(A-1)}$$

where V_{o} and V_{w} are the volumes of oil and water with relaxation time T_2. The echo spacings $t_{e,k}$ for DE sequences depend on both echo and sequence number, for instance

$$\begin{aligned} t_{e,k} &= t_{e,l_p} \text{ for } j = 1,2 \\ t_{e,k} &= t_{e,s} \text{ for } j \geq 3 \text{ for all } p \end{aligned}, \quad \text{.....(A-2)}$$

where $t_{e,s}$ and $t_{e,lp}$ are the short echo spacing for the third and subsequent echoes and the measurement-dependent initial echo spacings, respectively, used in the DE data suite.

Least-squares estimates of the fluid volumes and the errors in the volumes can be found by minimization of the squared deviations of the measured echo amplitudes from the model values. That is, one minimizes the error function $E(V_0,V_{\mathrm{w}})$,

$$E(V_0,V_{\mathrm{w}}) = \sum_k [M_k - V_{\mathrm{o}} M_{\mathrm{o}}(k) - V_{\mathrm{w}} M_{\mathrm{w}}(k)]^2, \quad \text{.....(A-3)}$$

where the quantities $M_{\mathrm{o}}(k)$ and $M_{\mathrm{w}}(k)$ are defined by the equations

$$M_{\mathrm{o}}(k) = \exp\left(-\frac{j\,t_{e,k}}{T_2}\right) I(k,\lambda T_2) \quad \text{.....(A-4)}$$

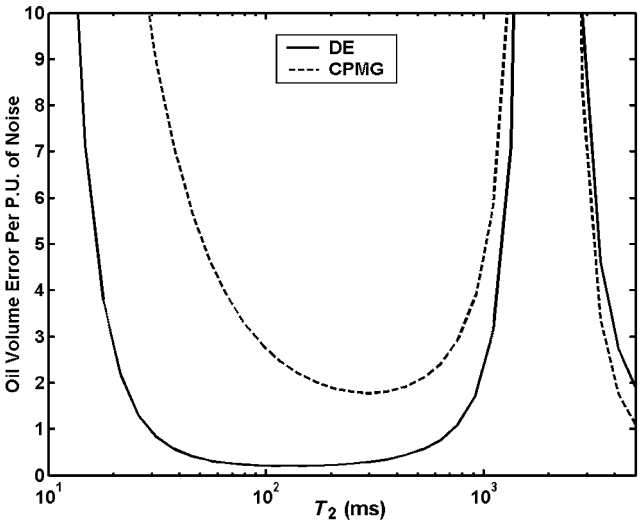

Fig. 14—Plot showing the standard deviations in the estimated oil volumes as a function of diffusion-free T_2 for suites of DE and CPMG data.

and

$$M_w(k) = \exp\left(-\frac{jt_{e,k}}{T_2}\right) I[k, D_w(T)] \quad \text{(A-5)}$$

Setting the first partial derivatives of $E(V_0, V_w)$ with respect to V_o and V_w equal to zero leads to the least-squares solution

$$V = A^{-1} * Q \equiv U * Q, \quad \text{(A-6)}$$

where we defined the column vectors $V = (V_o \; V_w)^T$ and $Q = (Q_o \; Q_w)^T$. The asterisk (*) denotes matrix multiplication and the superscript "T" denotes the transpose. The components of the Q vector are explicitly given by the equations

$$Q_o = \sum_k M_k M_0(k) \quad \text{(A-7)}$$

and

$$Q_w = \sum_k M_k M_w(k). \quad \text{(A-8)}$$

The elements of the 2×2 matrix A in Eq. A-6 are given by the equations

$$A_{1,1} = \sum_k M_0^2(k), \quad \text{(A-9)}$$

$$A_{1,2} = A_{2,1} = \sum_k M_0(k) M_w(k), \quad \text{(A-10)}$$

and

$$A_{2,2} = \sum_k M_w^2(k). \quad \text{(A-11)}$$

TABLE 5—CPMG DATA SUITE USED FOR SENSITIVITY ANALYSIS COMPUTATIONS

Measurement	TE (ms)	NE
1	0.4	5000
2	1.0	2000
3	2.0	1000
4	4.0	600
5	6.0	500
6	8.0	300
7	10.0	200
8	15.0	100
9	20.0	100
10	25.0	100

The matrix U in Eq. A-6 is the inverse of A. To save space, we do not display the matrix elements of U, which are easily calculated. Using the above results, the estimated volumes of water and oil having relaxation time T_2 are given by

$$V_o = U_{1,1} Q_o + U_{1,2} Q_w \quad \text{(A-12)}$$

$$V_w = U_{1,2} Q_o + U_{2,2} Q_w. \quad \text{(A-13)}$$

The standard deviations or errors in the estimated volumes are easily obtained from the previous equations. The errors come from the measurements M_k, and therefore from the vector Q in Eqs. A-12 and A-13. If we denote the noise per echo for all the measurements by σ_o and take the variance of both sides of the above equations, we find that the standard deviations in the oil and water volumes are given by

$$\sigma(V_0) = \sigma_0 [U_{1,1}^2 A_{1,1} + U_{1,2}^2 A_{2,2}]^{0.5} \quad \text{(A-14)}$$

$$\sigma(V_w) = \sigma_0 [U_{1,2}^2 A_{1,1} + U_{2,2}^2 A_{2,2}]^{0.5}. \quad \text{(A-15)}$$

In arriving at the above results, we have assumed that the noise on different echoes is uncorrelated.

The errors in the volume estimates have been computed for suites of DE and CPMG sequences. **Fig. 14** shows a comparison of the standard deviations in the oil volumes as a function of T_2 for suites of DE and CPMG data. The standard deviations shown in Fig. 14 were computed for data with 1.0 p.u. of random noise. The oil volume errors in Fig. 14 are proportional to the noise. Therefore, to compute the errors for data with 2.0 p.u. random noise, one would simply multiply the oil volume errors in Fig. 14 for both curves by a factor of two. The DE data suite that was used for the experiments in this paper was also used for the computations in this Appendix. The CPMG data suite shown in **Table 5** was used for the CPMG computations. Column 3 of the table shows the number of echoes (NE) used for each CPMG measurement. A gradient of 13.2 g/cm and a temperature of 25°C were used. It is clear from Fig. 14 that there are large errors in the estimated oil volumes for both short and long T_2 for the reasons discussed at the beginning of this Appendix. The errors are smaller for the DE data suite than for the CPMG suite for the reasons discussed in the paper. Observe that the errors actually decrease for very long T_2. The reason is that this is the regime of very light oils and condensates. There is good diffusion contrast, because hydrocarbon dif-

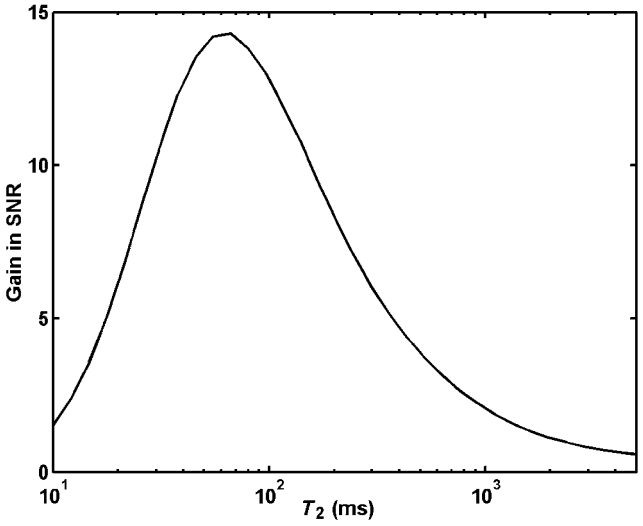

Fig. 15—The gain in measurement signal-to-noise ratio as a function of diffusion-free T_2 achieved by using DE data suites in place of CPMG data suites. Note that the gain is independent of the noise level, provided that the same noise is used for both the DE and CPMG data suites.

fusivities can be significantly greater than that of water for very long T_2 values.

Fig. 15 shows the ratio of the oil volume error for the CPMG data suite to the error for the DE data suite as a function of diffusion-free T_2. This ratio represents the "gain" in measurement signal-to-noise ratio that is achieved from using DE data suites in place of CPMG data suites. Note that the gain is independent of the noise level.

SI Metric Conversion Factors

°API	141.5/(131.5 + °API)		= g/cm
cp ×	1.0*	E–03	= Pa·s
cycles/s ×	1.0*	E+00	= Hz
ft ×	3.048*	E–01	= m
°F	(°F + 459.67)/1.8		= K
in. ×	2.54*	E+00	= cm

*Conversion factor is exact.

Robert (Bob) Freedman is a scientific advisor in the Reservoir Dept. at the Schlumberger Sugar Land Product Center. E-mail: freedman1@slb.com. He has 28 years of experience in formation evaluation, including five years with Shell, 5 years as an independent consultant, and 18 years with Schlumberger. Freedman holds an BS degree in physics from the U. of Houston, and a PhD degree in physics from the U. of California at San Diego. He has been an active member of SPE for 27 years, and served as an associate technical editor of the *SPE Formation Evaluation* journal from 1990–1992. Freedman is also a Distinguished SPE Lecturer (2003–2004). **Nicholas Heaton** joined the Schlumberger Sugar Land Product Center as NMR interpretation-development products specialist in 1998. e-mail: heaton2@slb.com. Previously, he worked in research at the U. of California at San Diego and the U. of Stuttgart. Heaton holds a BSc degree from the U. of Leeds, and a PhD degree in chemistry from the U. of Southampton. **Mark Flaum** is currently pursuing a doctorate in the Chemical Engineering Dept. at Rice U. e-mail: mflaum@rice.edu. His research focuses on the use of NMR diffusion-based measurements for characterization of porous media. Mark has co-authored 4 SPE papers on NMR fluid characterization and well-logging applications. Flaum holds a BEng degree in chemical engineering from McGill U. **George J. Hirasaki** had a 26-year career with Shell Development and Shell Oil Cos. before joining the Chemical Engineering faculty at Rice U. in 1993. e-mail: gjhirasaki@rice.edu. His research interests are in NMR well logging, reservoir wettability, enhanced oil recovery, gas hydrate recovery, asphaltene deposition, emulsion coalescence, and surfactant/foam aquifer remediation. He is a member of the National Academy of Engineering. Hirasaki holds a BS degree in chemical engineering from Lamar U. and a PhD degree in chemical engineering from Rice U. He was named an Improved Oil Recovery Pioneer at the 1998 SPE/DOR IOR Symposium and was the 1989 recipient of the Lester C. Uren Award. **Charles Flaum** is currently a scientific advisor at Schlumberger-Doll Research. e-mail: flaum@ridgefield.sdr.slb.com. He joined Schlumberger in 1977 as a Wireline Field Engineer, logging in the south-central U.S. His 26-plus-year career at Schlumberger includes over 10 years in research, six years in engineering centers, and 10 years in various field assignments in the U.S. and overseas. He has specialized in nuclear logging, magnetic resonance logging, general petrophysical interpretation, and thin bed evaluation. He holds a BSc degree from McGill U., and a PhD degree in nuclear physics from the U. of Rochester. **Martin Hürlimann** is a principal research scientist and manager of the NMR program at Schlumberger-Doll Research. e-mail: hurlimann@ridgefield.sdr.slb.com. Following a 2-year stay at the U. of California, Berkeley, in 1992 he joined Schlumberger, where he has worked on the development of new advanced NMR techniques. Hurlimann holds a degree from the Swiss Federal Inst. of Technology in Zürich, and a PhD degree in physics from the U. of British Columbia.